Frequency shifting with local nonlinearity management in nonuniformly poled quadratic nonlinear materials

K. Beckwitt, F. Ö. Ilday, and F. W. Wise

Department of Applied and Engineering Physics, Cornell University, Ithaca, New York 14853

Received October 7, 2003

We show theoretically that the frequency shifts that result from phase-mismatched cascaded processes under conditions of strong group-velocity mismatch can be significantly enhanced by local control of the nonlinearity with propagation. This control is possible with continuous variation of the poling period of quasi-phase-matched structures and can allow one to avoid saturation of the frequency shift. We theoretically demonstrate its applicability to high-quality, efficient frequency shifting of infrared pulses. © 2004 Optical Society of America

OCIS codes: 190.2640, 190.0190, 190.5650, 190.7110, 230.3990, 320.5540.

In recent years the nonlinear phase shifts that result from cascaded interactions in quadratic [$\chi^{(2)}$] nonlinear media have received much attention as a route to large nonlinear phase shifts of controllable magnitude and sign.[1] In particular, they have been shown to support the generation of solitons[2] and to compensate for Kerr phase shifts[3] and have proved useful for applications such as mode locking of short-pulse lasers, pulse compression,[4] and nonlinearity management for high pulse energies from fiber lasers.[5]

However, to date, applications of cascaded quadratic phase shifts to femtosecond pulses have been in the stationary limit, where the fundamental (FF) and the second-harmonic (SH) fields overlap temporally despite group-velocity mismatch (GVM) between them, producing an effective Kerr nonlinearity in the limit of large phase mismatch,[6] i.e., providing a surrogate for the bound-electronic cubic [$\chi^{(3)}$] nonlinearity.

Recently, nonstationary cascaded phase shifts were demonstrated.[7] GVM retards or advances (depending on its sign) the SH propagation with respect to the FF. Consequently, the resulting nonlinear phase shift imparted on the FF is advanced or delayed with respect to the stationary phase by an amount depending on the ratio of the GVM to the phase mismatch. This noninstantaneous nonlinear response manifests spectrally as redshifts or blueshifts of the pulse spectrum, which produces an analog of nuclear (Raman) nonlinearities from the quadratic process.[7]

In this Letter we propose a significant new degree of freedom for nonstationary cascaded frequency shifts: enhancement and control through local nonlinearity management in quasi-phase-matched (QPM) quadratic structures. Local nonlinearity control is achieved by aperiodically varying the QPM domain reversal period (to be discussed below). This added level of control greatly increases the applications of cascaded frequency shifts to frequency-shifting processes in the infrared.

We begin by reviewing the origin of cascaded frequency shifts.[7] Within the slowly varying envelope approximation, the coupled equations governing the interaction of the FF (a_1) and SH (a_2) field envelopes propagating in the z direction in a medium with quadratic nonlinearity under conditions of type I second-harmonic generation (SHG) are[8]

$$i\frac{\partial a_1}{\partial \xi} - \frac{\delta_1}{2}\frac{\partial^2 a_1}{\partial \tau^2} + {a_1}^* a_2 \exp(i\beta\xi) = 0\,, \quad (1)$$

$$i\frac{\partial a_2}{\partial \xi} - \frac{\delta_2}{2}\frac{\partial^2 a_2}{\partial \tau^2} - i\frac{\partial a_2}{\partial \tau} + {a_1}^2 \exp(-i\beta\xi) = 0\,. \quad (2)$$

Here, time is normalized to the initial pulse duration, $\tau = t/\tau_0$, the propagation coordinate is $\xi = z/L_{\mathrm{GVM}}$, and $\delta_j = L_{\mathrm{GVM}}/L_{\mathrm{DS},j}$ with dispersion lengths $L_{\mathrm{DS},j} = {\tau_0}^2/\mathrm{GVD}(\omega_j)$ (where GVD is group-velocity dispersion). $\beta = \Delta k L_{\mathrm{GVM}}$ for $\Delta k = k_{2\omega} - 2k_{\omega}$ (the FF–SH wave-vector mismatch), and $L_{\mathrm{GVM}} = \tau_0/(n_{1,g} - n_{2,g})$ for material group-velocity index $n_{j,g}$ with $j = 1, 2$.

In Refs. 7 and 9 it was shown that reducing Eqs. (1) and (2) to a single field equation for the FF through expansion in powers of β and keeping the lowest-order correction from GVM yields

$$\underbrace{i\frac{\partial a_1}{\partial \xi} - \frac{\delta_1}{2}\frac{\partial^2 a_1}{\partial \tau^2} - \frac{1}{\beta}\left(|a_1|^2 a_1\right)}_{\mathrm{NLSE}} + \underbrace{2i\frac{1}{\beta}|a_1|^2\frac{\partial a_1}{\partial \tau}}_{\mathrm{Correction}} = 0\,, \quad (3)$$

which consists of two parts: a standard nonlinear Schrödinger equation and the next-higher-order correction, which is responsible for the noninstantaneous phase shift that results from GVM in the nonstationary limit. In Ref. 7 it was shown that the correction qualitatively acts similarly to a Raman-scattering term [of the form[10] $(T_R a_1 \partial|a_1|^2/\partial\tau)$]. In analogy to Raman-scattering response time T_R, we define an effective response ${T_R}^{\mathrm{eff}} \sim i/\beta$ for the cascaded process.

This effective cascaded response has two effects: first, it is imaginary (unlike the Raman response), so it alters the field envelope instead of contributing directly to the phase. The envelope change couples to the phase profile through the remaining terms of Eq. (3), generating a Raman-like frequency shift through a higher-order process. Second, the frequency shifting saturates with $1/\beta \sim 1/\Delta k(\lambda)$: as the pulse's frequency shifts, Δk changes, eventually

0146-9592/04/070763-03$15.00/0

saturating the shift. In bulk materials with birefringent phase matching, where the dependence of Δk on λ is fixed, this saturation is unavoidable and limits the maximum achievable frequency shift.

Consider instead QPM materials in which phase matching is achieved through periodic reversal of the nonlinear tensor element along the direction of propagation. This allows precise control of Δk through control of the local nonlinear domain reversal period Λ. To date, researchers have used QPM structures with constant Λ to achieve highly efficient SHG in the visible and infrared frequencies[11] and structures with varying $\Lambda(z)$ (so-called chirped structures) to control the effects of dispersion in quadratic materials,[12] resulting in compressed SHG output. In these works the effects of grating chirp have been utilized for linear effects in propagation and in the context of phase-matched SHG.

We propose the use of continuously chirped QPM structures for phase-mismatched SHG as a way to alter the effective nonlinearity experienced by the pulse as it propagates. This can be achieved with z-dependent Λ, designed to control the effective Δk between the FF and the SH, and hence the local nonlinearity. Nonlinearity control is a new degree of freedom in the design and optimization of nonlinear processes in quadratic materials and has been considered for switching applications[13] and soliton formation.[14,15] Here we show that continuous nonlinearity control with chirped QPM gratings, combined with the effective Raman-like response described above, allows highly accurate optimization and control of cascaded frequency shifts. In QPM the net phase mismatch is given by $\Delta k_{\mathrm{net}}(\lambda, z) = \Delta k_{\mathrm{mat}}(\lambda) - 2\pi/\Lambda(z)$, where Δk_{mat} is the wavelength-dependent material phase mismatch. Hence, a pulse propagating in a structure with $\Lambda(z)$ designed to keep Δk_{net} constant with shifting FF wavelength will experience continued frequency shift (analogous to real Raman-frequency shift), avoiding saturation from the cascaded process.

Simulations of 100-fs, 0.6-μJ (15-GW/cm^2) pulses at 1550 nm propagating in chirped periodically poled lithium niobate (C-PPLN, $d_{\mathrm{eff}} \simeq 30$ pm/V; see Ref. 16), with and without chirp to optimize the nonlinear frequency shift appear in Fig. 1. Equations (1) and (2) are solved numerically with a symmetric split-step beam propagation method.[3] Λ is assumed to vary linearly, i.e., linear chirped QPM is assumed.

Figure 1 shows enhanced effective Raman shifts with period chirping. The resulting fields, which undergo continued shift with chirped poling, are the qualitative analog of Raman solitons. These cascaded Raman-like solitons provide a means of self-frequency shifting fixed frequency sources by many times their bandwidth. Additionally, the process provides a way to shift to lower wavelengths (i.e., the analog of anti-Stokes Raman shifts). High spectral and temporal quality can be achieved by removal of the unwanted frequencies with an edge filter. Figure 2 shows a 100-fs, 0.12-μJ (15-GW/cm^2) pulse at 1550 nm shifted by >200 nm in a C-PPLN structure (from $\Lambda = 38$ μm to 22 μm) with output quality factor 0.96 [Q, the ratio of energy within the full width at half-maximum (FWHM) of the pulse to that of the initial pulse]. As with ordinary Raman solitons, the cascaded soliton is temporally compressed, so its peak power is similar to that of the launched pulse.

This processes should be applicable to other wavelengths in the infrared, in particular, the technologically important 1030–1060-nm band, where high-energy sources exist. The only practical limits are that the wavelength must be suitable for material poling and the material parameters must support the shifting process (i.e., with short pulses, the sign of the group-velocity dispersion determines the direction of the shift, and the GVM cannot be too large). The ability to generate large and efficient frequency shifts with a clean pulse output is of great interest, since it presents an alternative to common optical frequency-conversion schemes such as optical parametric amplification but in a more compact and simple implementation.

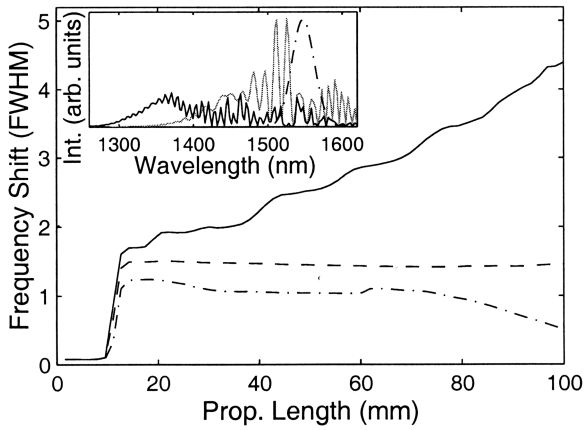

Fig. 1. Average spectral shift (in units of the initial FWHM, ~4.4 THz) with propagation. The dashed curve shows the linear shift followed by saturation with constant Λ. The solid (dashed–dotted) curve shows the shift with chirped structure to optimize (hinder) the spectral shift. Inset, input spectrum (rescaled, dashed–dotted curve) and shifted spectra with (black) and without (gray) period chirp.

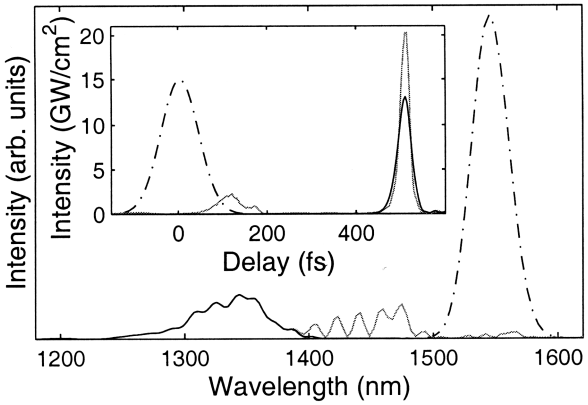

Fig. 2. Spectra and (inset) temporal profile of the input pulse (dashed–dotted) and shifted pulse before (gray curve) and after (black curve) filtering. Filtering reduces the output pulse energy from 48% to 33% of that launched but yields a pulse with $Q = 0.96$. The C-PPLN sample length is 4.6 cm.

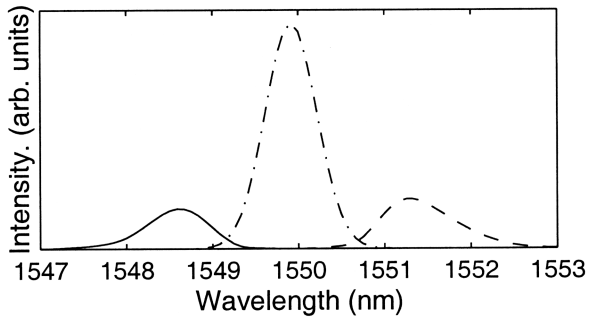

Fig. 3. Frequency shift of 5-ps, 50-pJ pulses in waveguided C-PPLN. The dashed–dotted curves show the input spectrum. The solid (dashed) curve shows the downshift (upshift) with a grating chirp of 18.425 to 18.405 μm (18.36 to 18.38 μm), after filtering out the unshifted frequency components. The waveguide dimensions are 3 μm by 7 μm.

For C-PPLN in the infrared, the sign of group-velocity dispersion is normal, preventing shifts to longer wavelengths with short pulses ($<\sim$picoseconds). However, with longer pulses (so dispersion is negligible) this restriction is lifted. This applies to high-bit-rate telecommunications applications, where the small modal area (and resulting high effective nonlinearity) available in waveguided periodically poled lithium niobate can be used to generate frequency shifts useful for wavelength-division multiplexing applications. Figure 3 shows shifting of 5-ps, 50-pJ pulses at 1550 nm in C-PPLN optimized for $\sim$1.5-nm upshift and downshift (one wavelength-division multiplexing channel). The resulting upshifted (downshifted) pulse contains 29% (19%) of the launched energy with Q of 0.94 (0.92).

Although the applications discussed above all pertain to tailoring $\Lambda(z)$ for optimized frequency shift, it should also be possible to modify the grating structure to affect the temporal profile of the output pulse. This could, for example, be used to maximize compression of the frequency-shifted FF, yielding output with higher peak power. Although it was not investigated here, one could consider algorithms for local pulse optimization, so that at any point in propagation the local structure is that needed to compress the field at that point [i.e., with more advanced functional forms of $\Lambda(z)$ than the linear case considered here]. Although it is beyond the scope of this Letter, this prospect warrants further study.

In conclusion, we have theoretically demonstrated the use of local nonlinearity control by poling-period variation in QPM quadratic interactions to optimize frequency shifting. This new degree of freedom increases the efficiency and quality of frequency shifts from cascaded processes and completes the analogy of cascaded frequency shifts to Raman-induced shifts by allowing an effectively constant response time for the cascaded process. As an example, we have theoretically shown clean and efficient frequency shifting of submicrojoule, $\sim$100-fs pulses by hundreds of nanometers, and we have shown the applicability of this shifting to wavelength-division multiplexing channel switching with pulse parameters representative of telecommunications systems in waveguided C-PPLN structures. We expect quadratic frequency shifting, enhanced with nonlinearity management, to have broad applications. Furthermore, this new capability can be easily customized and can be implemented with existing fabrication techniques.

This work was supported by the National Science Foundation (awards PHY-0099564 and ECS-0217958) and the National Institutes of Health (grant EB002019). K. Beckwitt's e-mail address is kb77@cornell.edu.

References

1. G. I. Stegeman, R. Schiek, L. Torner, W. Torruellas, Y. Baek, D. Baboiu, Z. Wang, E. Van Stryland, D. J. Hagan, and G. Assanto, in *Novel Optical Materials and Applications*, I. C. Khoo, F. Simoni, and C. Umeton, eds. (Wiley, New York, 1997), Chap. 2, pp. 49–76.
2. A. V. Buryak, P. Di Trapani, D. V. Skryabin, and S. Trillo, Phys. Rep. **370,** 63 (2002).
3. K. Beckwitt, F. W. Wise, L. Qian, L. A. Walker, and E. Canto-Said, Opt. Lett. **26,** 1696 (2001).
4. F. Wise, L. Qian, and X. Liu, J. Nonlinear Opt. Phys. Mater. **11,** 317 (2002).
5. F. Ö. Ilday and F. W. Wise, J. Opt. Soc. Am. B **19,** 470 (2002).
6. C. R. Menyuk, R. Schiek, and L. Torner, J. Opt. Soc. Am. B **11,** 2434 (1994).
7. F. Ö. Ilday, K. Beckwitt, Y.-F. Chen, H. Lim, and F. W. Wise, J. Opt. Soc. Am. B **21,** 376 (2004).
8. A. A. Kanashov and A. M. Rubenchik, Physica D **4,** 122 (1981).
9. J. P. Torres and L. Torner, Opt. Quantum Electron. **29,** 757 (1997).
10. G. P. Agrawal, *Nonlinear Fiber Optics* (Academic, San Diego, Calif., 1995).
11. M. M. Fejer, G. A. Magel, D. H. Jundt, and R. L. Byer, IEEE J. Quantum Electron. **28,** 2631 (1992).
12. A. M. Schober, G. Imeshev, and M. M. Fejer, Opt. Lett. **27,** 1129 (2002).
13. M. Cha, Opt. Lett. **23,** 250 (1998).
14. S. Carrasco, J. P. Torres, L. Torner, and R. Schiek, Opt. Lett. **25,** 1273 (2000).
15. S. C. Rodriguez, J. P. Torres, L. Torner, and M. M. Fejer, J. Opt. Soc. Am. B **19,** 1396 (2002).
16. G. Imeshev, M. M. Arbore, M. M. Fejer, A. Galvanauskas, M. Fermann, and D. Harter, J. Opt. Soc. Am. B **17,** 304 (2000).